NEW VIEWPOINTS IN MASS FILTER DESIGN

*MELVIN H. FRIEDMAN, PhD
US ARMY MOBILITY EQUIPMENT R&D COMMAND, FORT BELVOIR, VA 22060

JOSEPH E. CAMPANA, PhD
US NAVAL RESEARCH LABORATORY, WASHINGTON, DC 20375

ALFRED L. YERGEY, PhD
NATIONAL INSTITUTES OF HEALTH, BETHESDA, MD 20205

1. INTRODUCTION

The quadrupole mass filter (QMF) is ubiquitous in military and civilian mass spectrometry laboratories. This instrument is used by chemists to determine the mass distribution associated with a sample. As illustrated in figure 1, a QMF has four pole pieces and each of these is carefully shaped to follow the equation of a hyperbola i.e. with the co-ordinate system shown the equations of the pole pieces are given by $(x^2 - y^2) = \pm r_o^2$. In a typical QMF, r_o and ℓ are .28 cm and 15 cm respectively (1). Detailed analysis shows (2) that mass filtering action is achieved by imposing a voltage difference $\phi = \phi_{DC} - \phi_{AC} \cos \omega t$ between adjacent electrodes. The driving frequency $\nu = (\omega/2\pi)$ is typically 2.5 MHz. The voltages ϕ_{DC} and ϕ_{AC} are refered to as the DC and AC components of the applied voltage respectively. The result of detailed analyses (1,2) is that the mass resolution of a QMF is determined by the ratio ϕ_{DC}/ϕ_{AC} while the absolute magnitude of the voltages ϕ_{DC} and ϕ_{AC} determine the mass of the ion which sucessfully traverses the length of the instrument. In the typical operation of the instrument (1) ϕ_{DC} and ϕ_{AC} are allowed to vary while their ratio is held constant and the number of ions which sucessfully traverse the filter are recorded.

The mass resolving power of a mass filter at mass m is defined by $m/\Delta m$ where Δm is a measure of the smallest difference in mass at mass m that can be detected by the instrument at a specified valley (e.g. 10% peak height) between peaks of equal heights. The transmission of a mass filter tuned to mass m is defined as the ratio of the number of ions with mass m injected into the mass filter to the number which arrive at the detector. It would be desirable for a QMF to have high resolving power and high transmission. Unfortunately, these are conflicting requirements and the improvement in one of these parameters results in a degradation of the other parameter.
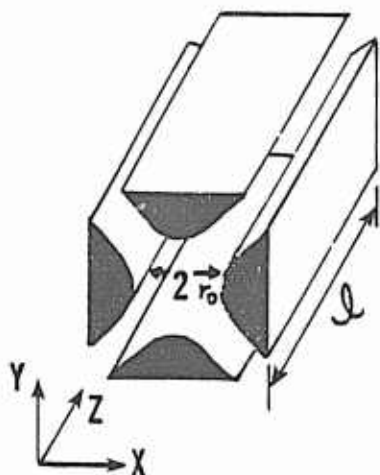
Figure 1. Electrode structure of the quadrupole and its relationship with the cartesian coordinate system. The coordinate system is oriented as shown but translated so that the origin is centered between the pole pieces as in figure 3. The ions, which move in a vacuum are introduced with a small velocity at x=0, y=0 in the z direction. By imposing a voltage difference with DC and AC components on adjacent electrodes the device is tuned so that only ions with the proper mass to charge ratio traverse the length of the filter where they are detected. Ions with a different mass to charge ratio collide with the electrode walls and are lost.
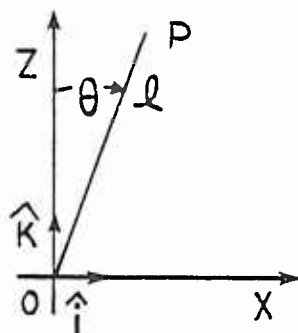

Figure 2. Inverted pendulum. The rigid rod OP of length ℓ is free to rotate in the x-z plane. The z-axis is oriented so it points away from the center of the earth and the support point O has an acceleration of $-b\omega^2 \cos \omega t$. For a high enough frequency ω the inverted pendulum has the remarkable property of being stable in a vertical position with its center-of mass above its support point.

The research reported here is motivated by the following question: Can the shape of the pole pieces or the time dependence of the applied potential difference be changed in such a way as to improve the resolution-transmission relationship? In part 2 of this paper, differential equations of ion motion are derived for geometries which generalize the popular quadrupole geometry. By integrating these equations of motion, the suitability of these geometries for mass spectrometry can be investigated. Should calculation indicate a particular geometry is suitable, the question of whether or not it yields improved performance can be investigated experimentally. Part 3 of this paper deals with the relationship between the QMF and the inverted pendulum. The inverted pendulum, which consists of a rigid rod free to rotate in a vertical plane and whose point-of-support is made to vibrate vertically has the remarkable property of being stable in a vertical position with its center of mass above its support point, providing the support point oscillates above a critical frequency. In part 3 of this paper it is shown that the differential equations for an ion traversing a QMF and the differential equations

describing the motion of an inverted pendulum can be cast into the same form. In this way the inverted pendulum is shown to be a mechanical analog of the QMF. This aspect of the work is significant for three reasons: 1) The motion of an ion as it traverses a QMF cannot be physically seen. By observing the motion of an inverted pendulum one may better appreciate the subtleties involved in the way a quadrupole works and perhaps obtain a better sense of what is happening in this device. This may be of value to the person who tries to design a better mass filter. 2) The inverted pendulum has pedagogical value for explaining the operation of a QMF to students and has already been used for this purpose by one of the authors (A.L.Y). 3) By showing that the inverted pendulum and QMF are related subjects, it is possible that studies on one of them may shed light on the other.

The inverted pendulum has been described by several authors (3-10). Corben and Stehle (3) have modeled the inverted pendulum as a rigid rod while Landau and Lifshitz (4) have modeled it as a point mass attached to a rigid massless rod. Kapitza (5) has discussed the case of the pendulum when the amplitude of the sinusoidal oscillation of the suspension point is small in comparison to the length of the pendulum. He has also reported what appears to be the first operative pendulum with an oscillating support point (normal and inverted). Kalmus (6) has discussed the theory of the inverted pendulum with triangular excitation of the support point, and has reported an operative inverted compound pendulum. Mitchell (7) has applied a method of averaging to find the stability of an inverted pendulum for small amplitude high frequency oscillation, and Howe (8) has described a theory for the stability of an inverted pendulum driven by oscillations of a random nature. A square-wave model of the inverted pendulum has been recently described by Yorke (9). In a previous publication (10), Friedman et al. have observed that the inverted pendulum is a mechanical analog of the QMF.

Partial derivations of the differential equations for ion motion in a QMF are given by Campana (1) and also by Dawson (2). A derivation (starting from the Lorentz force law and the most general form of the Maxwell equations) for ion motion in multipole fields with a discussion of various approximations has been given by Friedman et al. (11).

2. ION MOTION IN MULTIPOLE FIELDS

a. _Fundamental physics of ion motion_. The force on an ion with charge e moving with velocity $\vec{v}$ through space in which there is an electric field $\vec{E}$ and a magnetic field $\vec{B}$ is given by the Lorentz force law

$$\vec{F} = e(\vec{E} + \vec{v} \times \vec{B}) . \tag{1}$$

The differential equation which describes the motion of an ion through a field is obtained from Newton's law of motion

$$\vec{F} = m \frac{d^2 \vec{r}}{dt^2} \quad .$$

(2)

It is necessary to compute the $\vec{E}$ and $\vec{B}$ fields caused by the time varying potential imposed on the pole pieces to find the motion of the ions from equations (1) and (2). These are computed from Maxwell's equations. If the charges on the ions and their associated current densities can be neglected for the purpose of computing the $\vec{E}$ and $\vec{B}$ fields acting on them, then in the vacuum region where the ions are moving Maxwell's equations are:

$$\vec{\nabla} \cdot \vec{E} = 0 \qquad\qquad \vec{\nabla} \times \vec{E} = -\frac{\partial \vec{B}}{\partial t}$$

$$\vec{\nabla} \cdot \vec{B} = 0 \qquad\qquad \vec{\nabla} \times \frac{\vec{B}}{\mu_o} = \frac{\partial}{\partial t}(\epsilon_o \vec{E}) \qquad .$$

(M1)

If the $\vec{E}$ and $\vec{B}$ fields are not changing with time then Maxwell's equations (M1) become:

$$\vec{\nabla} \cdot \vec{E} = 0 \qquad\qquad \vec{\nabla} \times \vec{E} = 0$$

$$\vec{\nabla} \cdot \vec{B} = 0 \qquad\qquad \vec{\nabla} \times \vec{B} = 0 \qquad .$$

(M2)

The applicability of the two forms of Maxwell's equations (M1) and (M2) to ion motion in a mass filter merits discussion. Maxwell's equations (M1) are a good approximation in the vacuum region enclosed by the pole pieces of a mass filter. As pointed out in the introduction, the voltages on the electrodes change at radio-frequencies resulting in $\vec{B}$ and $\vec{E}$ fields which also change at the same frequencies. Therefore, it is not obvious that Maxwell's equations (M2) can be used for the purpose of computing ion motion. The use of equations (M2) for this purpose can be understood through the following discussion. Equations (M2) predict (12) that $B_o = E_o/c$ where B_o and E_o are the maximum amplitudes of the $\vec{B}$ and $\vec{E}$ fields and c is the speed of light. Thus the $\vec{B}$ field in the Lorentz force law (1) exerts a negligible force on the ion compared to the $\vec{E}$ field, unless the ion is moving at a speed comparable to the speed of light. Campana (1) has shown that the fastest ions in a quadrupole mass filter are moving slowly ($v/c < 10^{-4}$) compared to the speed of light, even under extreme operating conditions. Therefore, it is not necessary to consider the $\vec{B}$ fields any further for the purpose of computing the force on an ion. The Lorentz force law (1) reduces to $\vec{F}=e\vec{E}$, while equations (M2) become:

$$\vec{\nabla} \cdot \vec{E} = 0 \qquad\qquad \vec{\nabla} \times \vec{E} = 0 \quad .$$

(M3)

The second of these equations (M3) is valid only for an alternating potential which has a frequency ν low enough such that

$$\lambda = \frac{c}{\nu} \gg \ell \quad . \tag{3}$$

That is, the wavelenth λ associated with the electromagnetic wave must be much greater than the length ℓ of the electrode structure. The necessity of equation (3) can be understood in the following way. If the wavelength does not satisfy equation (3) there is a possibility of standing waves (just as in the case of sound waves in an organ pipe) and these are not predicted by equations (M3). Typically, the length of the mass filter is less than one meter and the frequencies used (1) are well below 10 MHz. Therefore equation (3) is well satisfied and equations (M3) can be used to compute the ion trajectory.

An $\vec{E}$ field which satisfies equation (M3) can be found with the aid of two mathematical theorems. Stokes theorem, valid for any continuous, differentiable vector field $\vec{A}$, asserts that

$$\int \int_S (\vec{\nabla} \times \vec{A}) \cdot d\vec{S} = \oint \vec{A} \cdot d\vec{r} \tag{4}$$

where $d\vec{r}$ is a vector on the circumference of the enclosed area S and whose direction is in the direction of integration. The vector $d\vec{S}$ has a magnitude equal to the area dS and its direction is normal to dS. The ambiguity in the two directions normal to dS is resolved by the right-hand rule, that is $d\vec{S}$ points in the direction of the thumb with the other fingers of the right hand pointing in the direction $d\vec{r}$. In equation (4), the integral on the right is over the entire circumference and the integral on the left is over the area S (not necessarily plane) enclosed by the circumference. Stokes theorem enables a two-dimensional integral over a surface which has the form on the left side of equation (4) to be evaluated by the simpler one-dimensional integral on the right-hand side of equation (4). Application of Stokes theorem to the second of equations (M3) implies

$$\oint \vec{E} \cdot d\vec{r} = 0 \tag{5}$$

over any closed path which defines a surface over which $\vec{\nabla} \times \vec{E} = 0$. The second mathematical theorem asserts that any vector field $\vec{E}$ which satisfies equation (5) around every closed path can be represented as the divergence of a scalar field $\phi(x,y,z)$, that is

$$\vec{E} = -\vec{\nabla}\phi(x,y,z) \quad . \tag{6}$$

Substituting $\vec{E}$ from equation (6) into the first of equations (M3) gives

$$\vec{\nabla} \cdot \vec{\nabla}\phi(x,y,z) = \nabla^2\phi(x,y,z) = 0 \quad . \tag{7}$$

The prescription for finding the differential equations of ion motion for any configuration of pole pieces can now be given. Let $f_i(x,y,z)$

denote the equation for the surface S_i of conductor i. The differential equation of motion can be found by first obtaining a potential function $\phi(x,y,z)$ which satisfies Laplace's equation (7) and which also satisfies the boundary conditions

$$\phi(x,y,z)\big|_{S_i} = \phi_i \quad . \tag{8}$$

Generally, it is difficult to find a function which satisfies equations (7) and (8). The function $\phi(x,y,z)$ can sometimes be found analytically using the method of images (12-14), or by complex variable theory (12-15), or by infinite series expansions (12-14,16) or it can be evaluated numerically using digital computers (17-19). Once the potential $\phi(x,y,z)$ is known, the differential equations of motion can be found using Newton's law

$$\vec{F} = m \frac{d^2\vec{r}}{dt^2} = -e\vec{\nabla}\phi(x,y,z) \quad . \tag{9}$$

As discussed earlier, this method is approximately valid for time-varying potentials

$$\phi_i = \phi_{DC} - \phi_{AC} \cos \omega t \tag{10}$$

providing the potential does not change too rapidly with time, i.e. subject to the limitations of equation (3). Physically, equation (10) corresponds to subjecting the electrodes to a voltage which has DC and AC components.

The remainder of this paper will consider only infinitely long conductors whose shape does not vary with z. Although real electrode structures must necessarily be of finite length, this approximation is made because it captures the essential features for the operation of electric RF devices while avoiding some of the mathematical complexities. With this approximation the potential for such a conductor configuration does not depend on z i.e. $\phi(x,y,z) = \phi(x,y)$ and hence the force in the z=direction is zero i.e. $m\,\ddot{z} = 0$. The equation of motion in the z-direction can be integrated directly

$$z = v_{z_0} t + z_0 \quad . \tag{11}$$

Here v_z and z_0 are the z-component of velocity and the z-coordinate respectively at t=0.

b. <u>Method of obtaining potential function and equations of ion motion in multipole fields</u>. The approach of the previous section was to find the potential function $\phi(x,y,z)$ for a specified set of conductors at potentials ϕ_i. An alternative approach is to find a function $U_n(x,y)$ which satisfies Laplace's equation (7) and from this function determine the equipotential surfaces of the pole pieces. If conductors with given applied potentials are fashioned which coincide with the equipotential

surfaces, a potential function

$$\phi(x,y) = K_n U_n(x,y) \tag{12}$$

can be found which satisfies Laplace's equation and the boundary conditions (8) by simply choosing the constant K_n properly. Physically, K_n is related to the dimension of the electrode structure and the applied electrode potentials; it is chosen such that $\phi(x,y)$ matches the known potentials at the equipotential surfaces.

Functions which satisfy Laplace's equation may be found by application of the theory of complex variables. If the complex variable $z = x + iy$ is raised to an integral power of n, then the result can be expressed as the sum of two functions, a real $U_n(x,y)$ and and imaginary $V_n(x,y)$ part:

$$(x + iy)^n = U_n(x,y) + iV_n(x,y) \quad . \tag{13}$$

The integer n defines the order of the multipole field. From complex variable theory z^n is known to be analytic and so the function $U_n(x,y)$ satisfies (15) Laplace's equation (7).

The method described here for obtaining the potential function and the differential equation of motion can be summarised as follows: raise the complex variable z to an integer power n to find a potential function which satisfies Laplace's equation (7) and the boundary conditions (8); then ion motion is found from Newton's Law of motion (9).

c. <u>Application</u> <u>to</u> <u>some</u> <u>multipole</u> <u>geometries</u>. The method described in section 2b will now be applied to the hexapole geometry. The function z^n is evaluated for n=3 to obtain

$$U_3(x,y) = x^3 - 3xy^2 \quad .$$

Since $\nabla^2 U_3(x,y) = 0$, the function $U_3(x,y)$ is the basis for a possible potential function in charge free space. Its equipotential surfaces are illustrated in figure 4. Each of the pole pieces have the same shape and so the structure is unchanged under a 60 degree rotation. The pole piece lying on the positive x-axis is chosen to have positive applied potential $+\phi_0/2$ to comply with convention (2) and the adjacent electrodes are chosen to have potential with the same magnitude but opposite sign. The potential function $\phi(x,y)$ which satisfies Laplace's equation and the boundary conditions is

$$\phi(x,y) = \frac{\phi_0}{2r_0^3} (x^3 - 3xy^2) \tag{16}$$

as is readily verified. With ϕ_0 given by equation (10), Newton's law becomes:
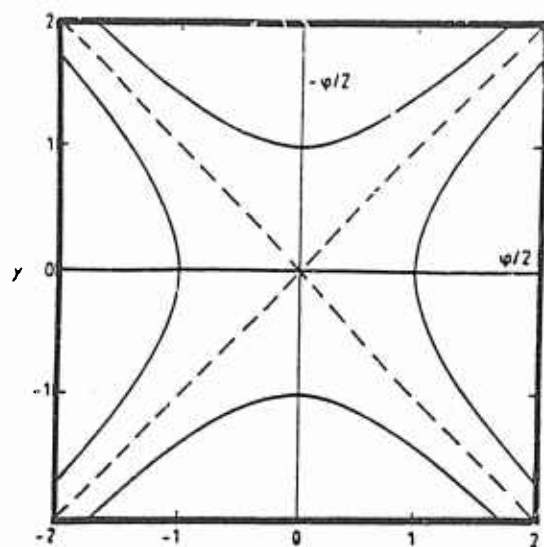
**FIGURE 3. QUADRUPOLE GEOMETRY.
EQUATION OF THE POLE PIECES:**

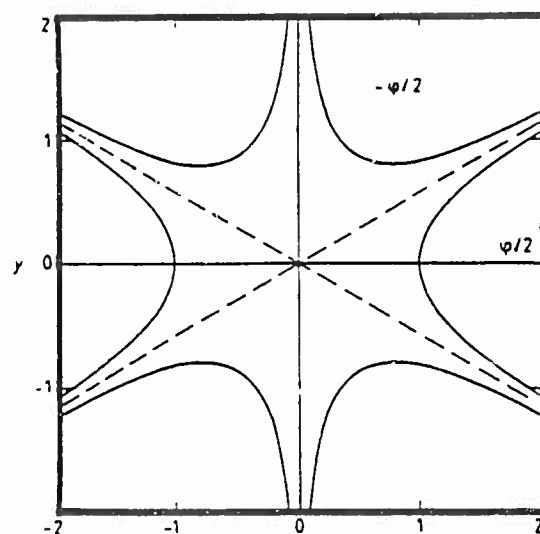$$\varphi(x, y) = (\varphi_0/2r_0^2)(x^2 - y^2).$$

**FIGURE 4. HEXAPOLE GEOMETRY.
EQUATIONS OF THE POLE PIECES:**

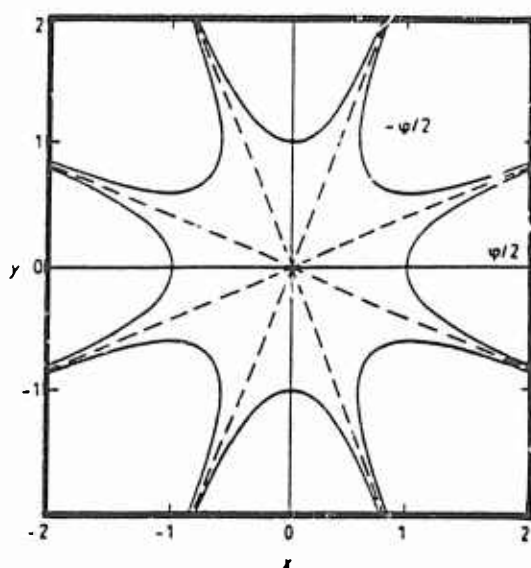$$\varphi(x, y) = (\varphi_0/2r_0^3)(x^3 - 3xy^2).$$

**FIGURE 5. OCTAPOLE GEOMETRY.
EQUATIONS OF THE POLE PIECES:**

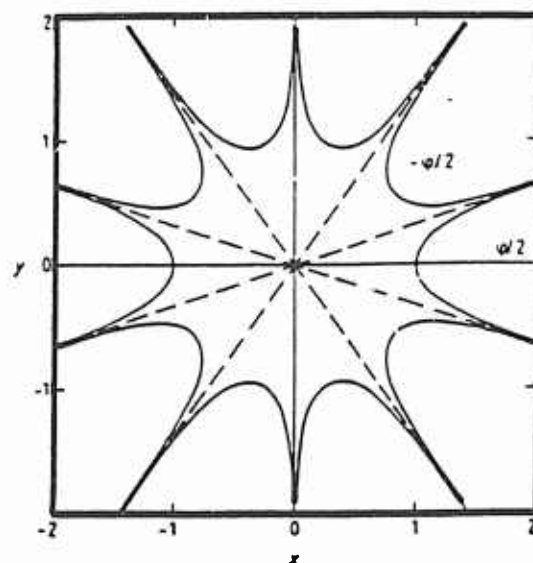$$\varphi(x, y) = (\varphi_0/2r_0^4)(x^4 - 6x^2y^2 + y^4).$$

**FIGURE 6. DECAPOLE GEOMETRY.
EQUATIONS OF THE POLE PIECES:**

$$\varphi(x, y) = (\varphi_0/2r_0^5)(x^5 - 10x^3y^2 + 5xy^4).$$

$$m \frac{d^2x}{dt^2} + \frac{3}{2} \frac{e}{r_o^3} (\phi_{DC} - \phi_{AC} \cos \omega t) (x^2 - y^2) = 0$$

$$m \frac{d^2y}{dt^2} - \frac{3e}{r_o^3} (\phi_{DC} - \phi_{AC} \cos \omega t) xy = 0 \quad .$$

$$(17)^*$$

The method just illustrated for n=3 determined the shape of the pole pieces (equation (16)) and the equations of ion motion (equation (17)) for the hexapole geometry. A similar procedure can be used for n any integer.

The geometry of the pole pieces when n=2 is the well-known quadrupole geometry illustrated in figures 1 and 3. The differential equation for ion motion in this case is:

$$m \frac{d^2x}{dt^2} + \frac{e}{r_o^2} (\phi_{DC} - \phi_{AC} \cos \omega t) x = 0 \tag{19a}$$

$$m \frac{d^2y}{dt^2} - \frac{e}{r_o^2} (\phi_{DC} - \phi_{AC} \cos \omega t) y = 0 \ . \tag{19b}$$

The geometry of the pole pieces when n=4 is illustrated in figure 5. The differential equation for ion motion in this case is:

$$m \frac{d^2x}{dt^2} + \frac{2e}{r_o^4} (\phi_{DC} - \phi_{AC} \cos \omega t) (x^3 - 3xy^2) = 0$$

$$m \frac{d^2y}{dt^2} - \frac{2e}{r_o^4} (\phi_{DC} - \phi_{AC} \cos \omega t) (3x^2y - y^3) = 0 \quad .$$

$$(20)^*$$

The geometry of the pole pieces when n=5 is illustrated in figure 6. The differential equation for ion ion motion in this case is:

$$m \frac{d^2x}{dt^2} + \frac{5e}{2r_o^5} (\phi_{DC} - \phi_{AC} \cos \omega t) (x^4 - 6x^2y^2 + y^4) = 0$$

$$m \frac{d^2y}{dt^2} - \frac{10e}{r_o^5} (\phi_{DC} - \phi_{AC} \cos \omega t) (x^3y - xy^3) = 0 \quad .$$

$$(21)^*$$

The method illustrated in these examples can easily be used for finding the differential equations of ion motion for n>5.

3. THE INVERTED PENDULUM AND THE QUADRUPOLE MASS FILTER

a. Theory of the inverted pendulum. In this section the differential equation of a rigid pendulum with vibrating support point is derived. Figure 2 shows the pendulum which is a thin solid rod of length ℓ and mass m tilted at angle θ with respect to the positive z-axis and whose point of support is moving with speed $\dot{Z}$ in the positive z direction. The equation of motion for the pendulum is found by use of the Lagrangian function L

where $L(q_k, \dot{q}_k) = T(q_k, \dot{q}_k) - V(q_k)$ and q_k, $\dot{q}_k$, T and V are the generalized coordinates, velocities, non-relativistic kinetic and potential energies respectively. The differential equation of motion is given by Lagrange's equation

$$\frac{d}{dt} \frac{\partial L(q_k, \dot{q}_k)}{\partial \dot{q}_k} - \frac{\partial L(q_k, \dot{q}_k)}{\partial q_k} = 0 \quad . \tag{22}$$

Consider the motion of the kth mass point m_k at distance ℓ_k from the support point. The velocity $\vec{v}_k$ of the mass point m_k is the vector sum of the velocity due to rotation and the velocity due to motion of the support point

$$\vec{v}_k = \frac{dx_k}{d\theta} \frac{d\theta}{dt} \hat{i} + (\frac{dz_k}{d\theta} \frac{d\theta}{dt} + \dot{z}) \hat{k} \quad .$$

The geometrical relationships

$$x_k = \ell_k \sin \theta \qquad\qquad z_k = \ell_k \cos \theta$$

allow $\vec{v}_k$ to be expressed in terms of the generalized coordinate θ and generalized velocity $\dot{\theta}$

$$\vec{v}_k = \ell_k \dot{\theta} \cos \theta \, \hat{i} + (\dot{z} - \ell_k \dot{\theta} \sin \theta) \, \hat{k} \quad . \tag{23}$$

Here $\hat{i}$ and $\hat{k}$ are unit vectors along the x and z axis respectively. Equation (23) and the definition of kinetic energy,

$$T = \frac{1}{2} \sum_k m_k v_k^2 = \frac{1}{2} \sum_k m_k \vec{v}_k \cdot \vec{v}_k \quad ,$$

allow the kinetic energy to be expressed in terms of the generalized coordinates and velocities

$$T = \frac{1}{2} (\sum_k m_k \ell_k^2) \, \dot{\theta}^2 - (\sum_k m_k \ell_k) \, \dot{\theta} \, \dot{z} \sin \theta + \frac{1}{2} m \, \dot{z}^2 \quad . \tag{24}$$

As seen from figure 2, the potential energy V of the pendulum in terms of each mass point m_k is a decreasing function of θ given by

$$V = (\sum_k m_k \ell_k) \, g \cos \theta \tag{25}$$

where g is the acceleration of gravity. Equations (24) and (25) may be simplified by using the definitions for the moment of inertia I of a body rotating about the support point and the coordinate of the center of mass ℓ_c measured from the support point along the axis of the rod:

$$I = \sum_k m_k \ell_k^2 \qquad\qquad \ell_c = \frac{1}{m} \sum_k m_k \ell_k \quad .$$

If the mass is distributed symmetrically about its mid-point, then $\ell_c = \ell/2$ and Lagrange's equation can be written

$$L = \frac{1}{2} I \dot{\theta}^2 + \frac{1}{2} m \dot{Z}^2 - m \frac{\ell}{2} \dot{\theta} \dot{Z} \sin \theta - mg \frac{\ell}{2} \cos \theta \quad . \tag{26}$$

With $q=\theta$, Lagrange's equation (22) applied to equation (26) yields the differential equation

$$I\ddot{\theta} - m \frac{\ell}{2} \ddot{Z} \sin \theta = mg \frac{\ell}{2} \sin \theta \quad . \tag{27}$$

Two simplifications of equation (27) can be made. First, the moment of inertia for a uniform thin solid rod is easily computed (10)

$$I = m \frac{\ell^2}{3} \quad .$$

Second, the approximation $\sin \theta = \theta$ is made since it is anticipated that the oscillations of the pendulum will be stable near $\theta=0$ and so $\sin \theta$ will be small. Making these two substitutions, equation (27) becomes

$$\ddot{\theta} - \frac{3}{2\ell} (g + \ddot{Z}) \theta = 0 \quad . \tag{28}$$

Equation (28), the principal result of section (3a), is seen to be reasonable if the cases $\ddot{Z}=0$, $\ddot{Z}=-g$ and $\ddot{Z}=+g$ are considered. For the case $\ddot{Z}=0$, equation (28) asserts that θ will grow exponentially with time constant $\tau = ((2\ell)/(3g))^{\frac{1}{2}}$. This is in agreement with the intuitive expectation that an inverted pendulum without oscillations is unstable. For the case $\ddot{Z}=-g$, the support point is moving down with a constant acceleration g. Equation (28) predicts that $\ddot{\theta}=0$ and this is in agreement with intuitive expectations since for a freely falling pendulum the effective forces acting to change the variable θ are expected to vanish. For the case $\ddot{Z}=+g$ the pendulum support point is accelerating upward with constant acceleration g. Equation (28) predicts that the motion for the variable θ is the same as that of a stationary pendulum sitting in a gravitational field of strength 2g and this too is in agreement with intuitive expectations.

b. The Mathieu equation. Subsequently it will be seen that the equation describing ion motion in a quadrupole and the equation describing the inverted pendulum can both be put in the cannonical form of the Mathieu equation. The purpose of this section is to describe this equation and its stability characteristics.

The canonical form of the Mathieu equation is

$$\frac{d^2 u}{d\xi^2} + (a - 2q \cos 2\xi)u = 0 \quad . \tag{29}$$

Here a and q are real constants, positive or negative, which are not functions of the dependent variable u or the independent variable ξ.
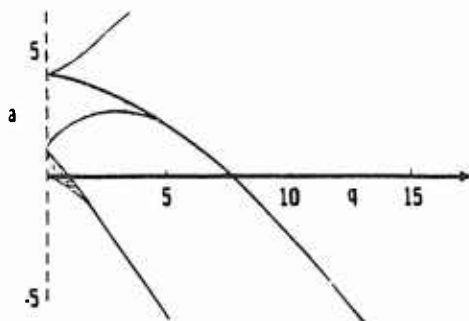
Figure 7. The a-q stability diagram. Equation (29) defines the parameters a and q which appear in the Mathieu equation. For a and q values which fall in the shaded area the value of u in equation 29 remains bounded as ξ increases independent of the initial conditions. Other values of a and q result in unbounded solutions.

Although the factor -2 multiplying q and the 2 in the argument of the cosine function might look strange, this is the standard for of this differential equation whose properties have been extensively studied.[22,23]

The solution of equation (29) will be a function of the form

$$u = u(\xi; a,q,u_o,\dot{u}_o) \ .\tag{30}$$

Equation (30) expresses mathematically the observation that the function u depends on the independent variable ξ, on the parameters a and q, on the initial value of u denoted by u_o, and on the initial value of $du/d\xi$ denoted by $\dot{u}_o$. The function (30) evaluated for a particular value of a and q is a function of ξ, u_o and $\dot{u}_o$. The result of detailed mathematical analysis (22) is that, depending on the values of the parameters a and q, the function u becomes unbounded or remains bounded as ξ increases and that these values of a and q are independent of the initial conditions u_o and $\dot{u}_o$. Figure 7 shows a portion of a stability diagram in a-q space. The shaded area results in "stable" trajectories by which it is meant that u remains within finite bounds as ξ increases independent of initial conditions.

c. Analogy between inverted pendulum and quadrupole mass filter. In this section it is shown that both the inverted pendulum and the QMF can be expressed in the cannonical form of the Mathieu equation and the analogs will be identified.

In equation (28) $\ddot{Z}$ is the acceleration of the support point. If the support point is driven sinusoidally with frequency ω, then the origin of time can be chosen so that $Z = b \cos \omega t$. In that case, equation (28) becomes

$$\frac{d^2\theta}{dt^2} - \frac{3}{2\ell} (g - b \ \omega^2 \ \cos \omega t) \ \theta = 0 \ \ .\tag{31}$$

Define four dimensionless parameters

(a) $u = \theta$ (b) $a = - \dfrac{6g}{\ell \omega^2}$

(c) $\xi = \dfrac{\omega t}{2}$ (d) $q = - \dfrac{3b}{\ell}$

$$\tag{32}$$

and use these to replace the variables ϑ and t in equation (31) to get the cannonical form of the Mathieu equation (29).

Note that equations (19a) and (19b) are essentially the same aside from a change in sign and so without loss of generality only equation (19b) is considered in drawing the analogy with the inverted pendulum. Define four dimensionless parameters

$$
\text{(a)} \quad u = y \qquad\qquad \text{(b)} \quad a = -\frac{4e\phi_{DC}}{m\omega^2 r_o^2}
$$

$$
\text{(c)} \quad \xi = \frac{\omega t}{2} \qquad\qquad \text{(d)} \quad q = -\frac{2e\phi_{AC}}{m\omega^2 r_o^2}
$$

(33)

and use these to replace y and t in equation (19b) to get the cannonical form of the Mathieu equation (29).

From equations (32) and (33) the analogous quantities can be identified. Multiplying numerator and denominator of equation (32b) by m, the mass of the pendulum, and comparing equations (32b) and (33b), aside from some unimportant numerical factors, the quantity mg of the pendulum is analogous to $(e\phi_{DC})/r_o$ of the QMF; $m\ell$ of the pendulum is analogous to mr_o of the QMF and ω of the pendulum is analogous to ω of the QMF. Multiplying numerator and denominator of equation (32d) by $m\omega^2$ and comparing equations (32d) and (33d), aside from some unimportant numerical factors, the quantity $bm\omega^2$ of the pendulum is analogous to $(e\phi_{AC})/r_o$ of the QMF; $m\ell$ of the pendulum is analogous to mr_o of the QMF and ω of the pendulum is analogous to ω of the QMF. In these analogies, all the quantities associated with the pendulum have the same physical dimensions as the corresponding quantities associated with the QMF. Also, the RF source of the QMF and the oscillating source for the support point in the inverted pendulum perform analogous functions of producing a stability mechanisim for each system. The destabilizing terms of each system are g, the acceleration of gravity for the inverted pendulum, and ϕ_{DC}, the applied DC voltage of the QMF. The quantities which counter these destabilizing terms are $b\omega^2$, the acceleration amplitude for the support point of the inverted pendulum and ϕ_{AC}, the RF amplitude of the QMF.

4. CONCLUSIONS.

Explicit differential equations in closed form have been found for pole piece geometries which are generalizations of those used in the QMF. For arbitrarily shaped pole pieces, the solution of Laplace's equation cannot be written in closed form and, thus in general the ion differential equations of motion cannot be written in closed form. The geometries shown in figures 4, 5 and 6 are analytically useful in determining if other geometries might yield mass filters with improved resolution/transmission characteristics. Computer simulation of ion motion in these geometries is a subject for future research.

Although not reported in this paper, an inverted pendulum has been built (10) and it has been useful in emphasizing to students the non-intuitive nature of the mass filtering action that takes place in a QMF. In reference (10), it is shown conceptually that the inverted pendulum can be used to experimentally measure the boundaries between the stable and unstable regions in the a-q stability diagram. As a result, the inverted pendulum aids in understanding these diagrams which are crucial to understanding the operation of a QMF.

The principal new results of our research are: 1) new derivations of the equations which describe ion motion in a QMF, 2) the equations of pole pieces for hexapole, octupole and decapole geometries illustrated in figures 4, 5 and 6, 3) closed form differential equations of ion motion in these geometries (equations (17), (20) and (21)) and 4) the realization that the inverted pendulum is a mechanical analog of the QMF.

Today the quadrupole mass analyser is the most widely used mass analyser for low resolution applications. Typically, mass filters are used in laboratory environments where simplicity, compactness, economy, absence of magnetic fields, and/or the capability of fast scan rates (especially for chromatographic combinations) are important (1). Thus, an improvement in resolution/transmission qualities of electric RF mass filters would enable this widely used mass spectrometer to take a larger role in analytical laboratories and in basic research. Other design considerations besides resolution/transmission characteristics are important. If mass filters could be made which are smaller, more rugged, less susceptible to vibration with reduced power requirements, and more easily maintained, there might be greater application outside the laboratory. Possible applications include: surveying for natural resources, pin-pointing sources of industrial pollutants, and the detection of hazardous materials such as chemical agents and explosives. Eventually our work may be applied to the solution of these problems.

REFERENCES

1. J. E. Campana, Elementary Theory of the Quadrupole Mass Filter, Int. J. Mass Spectrom. Ion Phys. 33, 101 (1980).
2. P. H. Dawson (Ed), Quadrupole Mass Spectrometry and its Applications, Elsevier, Amsterdam (1976).
3. H. C. Corben and P. Stehle, Classical Mechanics, John Wiley and Sons, New York (1960).
4. L. D. Landau and E. M. Lifshitz, Mechanics, Pergamon Press. London (1960).
5. P. L. Kapitza, in D. ter Haar (Ed), Collected Papers of P. L. Kapitza, Pergamon Press, London (1965) pp 714, 726.
6. H. P. Kalmus, The Inverted Pendulum, Am. J. Phys. 38, 874 (1970).

7. R. Mitchell, Stability of the Inverted Pendulum Subjected to Almost Periodic and Stochastic Base Motion - An Application to the Method of Averaging, Int. J. Non-Linear Mech. 7, 101 (1974).
8. M. S. Howe, The Mean Square Stability of an Inverted Pendulum Subject to Random Parametric Excitation, J. Sound Vib. 32, 407 (1974).
9. E. C. Yorke, Square-Wave Model for a Pendulum With Oscillating Suspension, Am. J. Phys. 46, 285 (1978).
10. M. H. Friedman, J. E. Campana, L. Kelner, E. H. Seeliger and A. L. Yergey, The Inverted Pendulum: A Mechanical Analog of the Quadrupole Mass Filter, Am. J. Phys., in press.
11. M. H. Friedman, A. L. Yergey and J. E. Campana, Fundamentals of Ion Motion in Electric Radio Frequency Fields, J. Phys. E: Sci. Instr. 15, 53 (1982).
12. E. M. Pugh and E. W. Pugh, Principles of Electricity and Magnetisim, Addison-Wesley, Reading, MA (1960).
13. S. Ramo, J. R. Whinnery, T. van Duzer, Fields and Waves in Communication Electronics, John Wiley and Sons, New York (1965).
14. J. D. Jackson, Classical Electrodynamics, John Wiley, New York (1962).
15. R. V. Churchill, Complex Variables and Applications, McGraw-Hill, New York (1941).
16. R. V. Churchill, Fourier Series and Boundary Value Problems, McGraw-Hill, (1963).
17. K. J. Binns and P. J. Lawrenson, Analysis and Computation of Electric and Magnetic Field Problems, Macmillan, New York (1963).
18. M. G. Salvadori and M. L. Baron, Numerical Methods in Engineering, Prentice Hall, Englewood Cliffs, N.J. (1964).
19. V. Vemuri and W. J. Karplus, Digital Computer Treatment of Partial Differential Equations, Prentice Hall, Englewood Cliffs, N.J. (1981).
20. W. Paul and H. Steinwendel, A New Mass Spectrometer Without a Magnetic Field, Z. Naturforsch 8a, 448 (1953).
21. W. Paul. H. P. Reinhard, U. von Zahn, The Electric Mass Filter as Mass Spectrometer and Isotope Separator, Z. Phys. 152, 143 (1958).
22. N. W. McLachlan, Theory and Application of Mathieu Functions, Oxford University Press, London (1947).
23. M. Abramowitz and L. A. Stegun (Ed), Handbook of Mathematical Functions With Formulas, Graphs and Mathematical Tables, National Bureau of Standards, Applied Mathematics Series 55 (1964).